Deposition of Bone-Like Apatite on Modified Silk Fibroin Films From Simulated Body Fluid

Rikako Kino,[1,4] Toshiyuki Ikoma,[3] Akira Monkawa,[3] Shunji Yunoki,[3] Masanobu Munekata,[4] Junzo Tanaka,[1,3] Tetsuo Asakura[2]

[1]*Division of Frontier Research, Creative Research Initiative "SOUSEI" (CRIS), Hokkaido University, Kita 21, Nishi 10, Kita-ku, Sapporo 001-0021, Japan*
[2]*Department of Biotechnology, Tokyo University of Agriculture and Technology, Koganei, Tokyo 184-8588, Japan*
[3]*Biomaterials Center, National Institute for Materials Science, Namiki 1–1, Tsukuba, Ibaraki 305-0044, Japan*
[4]*Faculty and Graduate School of Engineering, Hokkaido University, Kita 13, Nishi 9, Kita-ku, Sapporo, 060-8628, Japan*

ABSTRACT: Silk fibroin films with various calcium chloride contents were prepared by a cast film method and subsequent MeOH treatment. The conformational changes from α-helix to β-sheet structure were analyzed by Fourier transformed infrared attenuated total reflection spectroscopy measurements. The films obtained were soaked in 1.5-times simulated body fluid (1.5 SBF) and the deposition of hydroxyapatite crystals were observed by scanning electron microscopy. The films with calcium chloride contents lower than 3 wt % relative to the silk fibroin were not mineralized under these conditions, while those with calcium chloride contents more than 5 wt % mineralized after 6 h. The X-ray diffraction patterns and inductive coupled plasma spectroscopy analyses indicated that the hydroxyapatite crystals were grown by hydrolysis of octacalcium phosphate, as indicated by differences in diffraction intensities and changes in concentrations of calcium and phosphate ions in 1.5 SBF. © 2005 Wiley Periodicals, Inc. J Appl Polym Sci 99: 2822–2830, 2006

Key words: silk fibroin; hydroxyapatite; composites; films; biomineralization

INTRODUCTION

Silk fibroin is a fibrous protein and a bioactive polymer with high mechanical strength, elasticity, and suppleness.[1] The natural undegummed silkworm fiber has a two silk fibroin twins, both surrounded by a sericin outer-layer.[1–3] Silk sutures, used in surgical, has shown an immune response in some cases probably due to contamination with sericin (glue-like protein).[1,4] The sericin is an allergen causing a Type I allergic response.[5] Recently, many authors have reported its biological reactions while the core silk fibroin shows in vitro and in vivo biocompatibility with collagen and synthetic polymers such as polylactic acid.[1,6] The silk fibroin is, thus, a potential biomaterial for scaffold in tissue engineering to produce artificial regenerating bone,[1,7–9] cartilage,[10] skin, and ligament[1,11–12] in vitro. It should be noted that the degummed silk without the sericin is favored for biomaterials for the reason stated earlier.

Absorption of silk suture in vitro has been described by many authors.[13–15] Lam et al.[16] have described the breakdown and absorption of degummed silk sutures in vivo. These showed initial signs of breakdown after 2 weeks implantation and, at 6 and 12 weeks, the fragmentation prevented the sutures being removed from the tissues. The sutures were completely degradated and absorbed by proteolytic enzymatic digestion. The absorption of silks depended on the morphology (fiber, film, sponge) and the content of three different conformations (α-helix, random coil, and β-sheet).[17] Control of conformation and morphology is, thus, of great importance for developing silk scaffolds for tissue engineering.

Fibroin films prepared by casting from aqueous solutions have been intensively studied for over a decade.[18–21] The bulk and surface structure of the films are key factors for improving mechanical properties and biological reactions. Thus, the effect of casting conditions, such as initial concentration, drying rate, pH, and temperature, on conformational change has been investigated.[22–24] The proportion of conformations can be correlated with absorption rates, determined from changes in tensile strength.[11,17,25,26]

The metal ions, such as calcium, copper, zinc, and potassium ions, influence the conformational transition from α-helix to β-sheet and/or β-sheet intermediates in cast silk fibroin films.[22,26] Zhou et al. studied the conformations of silk fibroin films prepared from
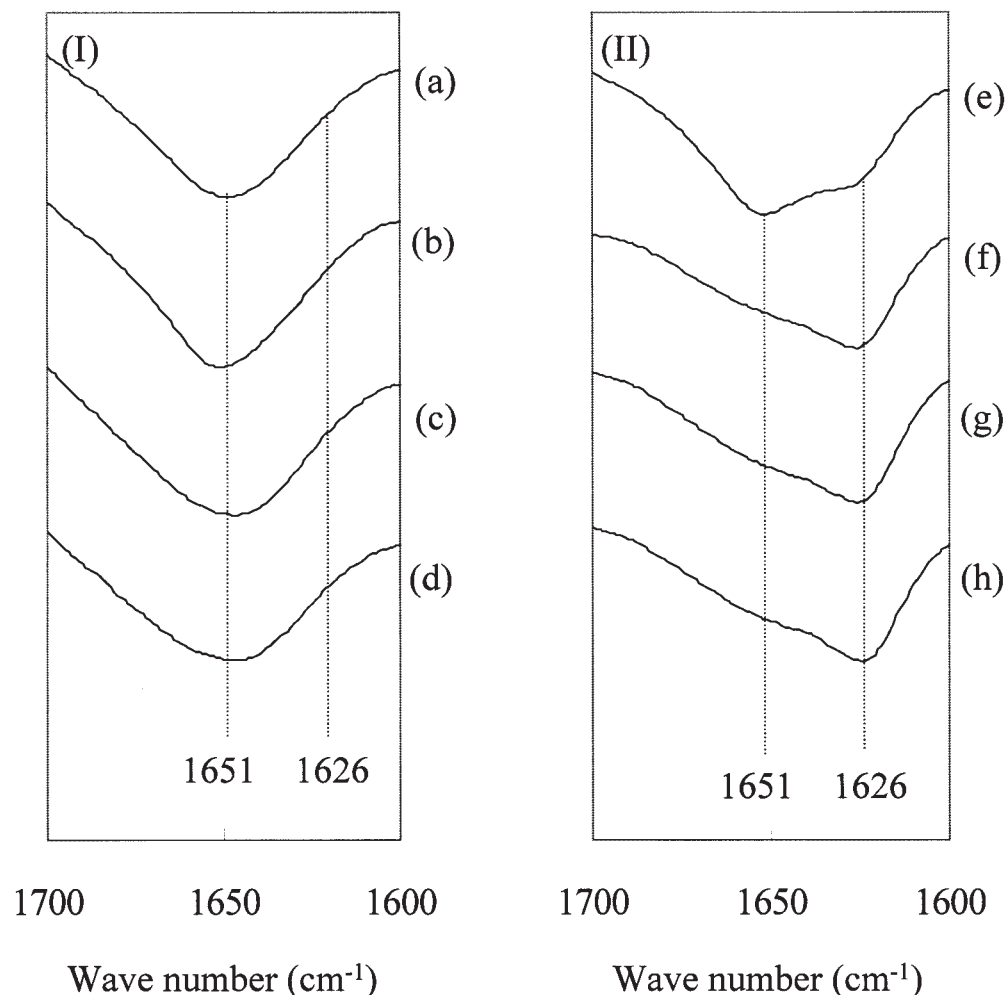

Figure 1 FTIR-ATR spectra of SFFs with various contents of calcium chloride (I) before and (II) after the MeOH treatment; (a) and (e) for SFF-0, (b) and (f) for SFF-3, (c) and (g) for SFF-5, and (d) and (h) for SFF-10.

the regenerated silk fibroin solutions with various calcium chloride contents and pHs (from pH 5.2 to 8.0). The addition of calcium ions at contents <10 wt % relative to the fibroin and high pH promoted the formation of "random coil" conformation. Li et al.[27] showed that metal ions at certain concentrations could promote the random coil to β-sheet transition of silk fibroin. The portion of hydrophobic chains probably became stable to bind calcium ions in low pH, of which structure is β-sheet or the intermediate, while concentrated solutions of calcium chloride and/or calcium nitrate in a mixture of water and ethanol can dissolve silk fibroin. The calcium ion was in general completely removed by the dialysis process in distilled water, and the deposition of hydroxyapatite on the surface from SBF has not been studied.

The calcium ion is a key cation in the formation of hydroxyapatite ($Ca_{10}(PO_4)_6(OH)_2$) crystals on polymer surfaces. Hydroxyapatite is also a bioactive ceramic directly bonded to the protein matrix in bone and teeth.[29–32] Artificial composites of hydroxyapatite and

natural biopolymers, such as collagen[33–39] and polysaccharides,[40] have been extensively studied to improve mechanical properties and biological reactions. Many authors have developed composites with covalently crosslinked silk-based materials and hydroxyapatite. A simulated body fluid (SBF)[9] and an alternative soaking method[41] have also been used for mineralization. The formation of hydroxyapatite on the surface from the SBF is thought to promote direct bonding to natural bone tissue in vivo.[42,43] The combination of the excellent properties of silk and hydroxyapatite can be useful for designing bone repair, tooth filling materials and/or cell-seeded scaffolds for tissue engineering.

In this study, we studied the deposition of hydroxyapatite crystals from a SBF on silk fibroin films prepared with and without calcium ions. The structures of cast films were determined by Fourier transformed infrared attenuated total reflection spectroscopy (FTIR-ATR). The deposition rate and changes in mineral structure were investigated by scanning electron
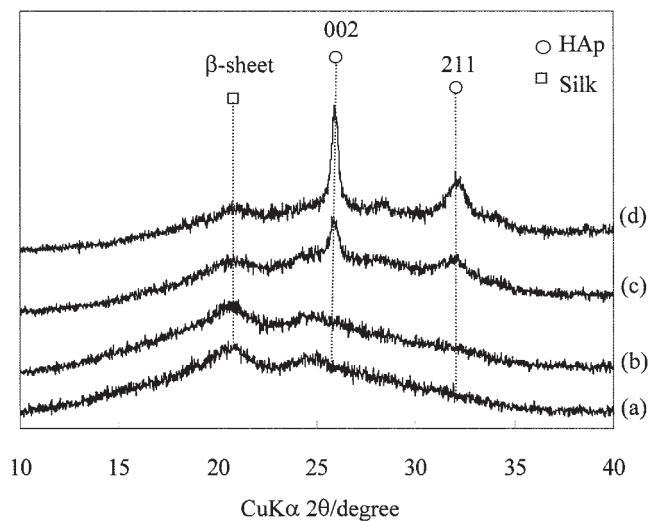
Figure 2 XRD patterns of SFFs after soaking into 1.5 SBF for 7 days; (a) SFF-0, (b) SFF-3, (c) SFF-5 and (d) SFF-10.

microscopy (SEM) and X-ray diffractometry (XRD). The elution of calcium ions from the cast silk fibroin films and the change of ion concentration in the SBF after soaking at various days were analyzed by inductive coupled plasma spectroscopy (ICP).

EXPERIMENTAL

Materials

The cocoon of *Bombyx mori* was degummed with three washes in fresh 0.5% (w/v) Marseilles soap solution at 100°C for 30 min, and finally, thoroughly washed with distilled water. The silk fibroin fiber was then dissolved in $9M$ LiBr (Wako Pure Chemical Industries) at 40°C[44] and was dialyzed with distilled water at room temperature for 4 days. The concentration of silk fibroin in the solution was measured accurately by drying the solution at 120°C for 3 h after dialysis. Calcium chloride was then added into the solution to give final contents of 0.0, 3.0, 5.0, and 10 wt % relative to silk fibroin. The pH values of the solutions were 6.98, 6.48, 6.15, and 5.95. The silk fibroin films were then prepared by casting on smooth polystyrene (PS) plates at room temperature (25°C) and constant humidity (50%). The films obtained were treated with MeOH vapor at room temperature for 2 days to make them water-insoluble. The silk fibroin films containing 0.0, 3.0, 5.0, and 10.0 wt % of calcium chloride were termed SFF-0, SFF-3, SFF-5, and SFF-10, respectively.

The ultraviolet (UV) spectra of the films were measured directly without the use of a cell by a UV–visible spectrophotometer (U-3500, Hitachi, Japan) at 500 nm in wavelength. The data were normalized to the thickness of 100 μm using Lambert's law after measuring the film thickness using a micrometer caliper. The

FTIR-ATR analysis was performed with Perkin–Elmer FT-IR8000 spectrophotometer. The conditions were as follows: resolution 4 cm^{-1}; 128 repeated scans; cast films 1×3 cm^2. The initial reflection elements were Ge prism with the incident angle of 45°.

Hydroxyapatite deposition on the silk fibroin surface from SBF

The silk fibroin films were soaked into 1.5 SBF prepared by dissolving $CaCl_2$, $NaHCO_3$, KCl, $K_2HO_43H_2O$, $MgCl_2$, $CaCl_2$, and Ns_2SO_4 in ultrapure water according to the method of Kokubo et al.,[45] and buffered at pH 7.25 with 75 mM $(CH_2OH)_3CNH_2$. The temperature of the solution was kept at 36.5°C for 3, 6, and 12 h, 1 day, 3, and 7 days. The films were washed with distilled water and dried at ambient temperature and constant humidity.

Structure and morphology of the deposited hydroxyapatite crystals

XRD recordings for the hydroxyapatite/silk composites were made at room temperature using a RINT-Ultimo III/C Rigaku diffractometer with graphite monochromatized CuKa radiation at 40 kV and 40 mA. The intensity data were collected in 0.1° steps over a 2θ range of $10-40°$

Film surfaces were observed at 10 or 3 kV using SEM of JMS 5600 after sputtering with platinum or tungsten.

Ion concentrations in both water and SBF after soaking the silk fibroin films

The elution of calcium ion in ultrapure water from the films was analyzed by ICP after soaking for 1, 3, 5, 10, 20, and 30 min and 2 days. The supernatant liquids were taken after soaking 400 mg of the films in 200 mL of ultrapure water at room temperature at $25 \pm 1°C$.

We also examined changes in Ca^{2+}, P as HPO_4^{2-}, Na^+, and K^+ concentrations at 1, 3, 6, 12, and 24 h in 1.5 SBF solution after soaking silk fibroin films (1 mg of film/mL 1.5 SBF) at 36.5°C. The compositions of the deposited hydroxyapatite on the silk surface were determined from the changes in the 1.5 SBF ion concentrations.

RESULTS AND DISCUSSION

The structural properties of silk fibroin films

The SFF-0, SFF-3, SFF-5, and SFF-10 had thickness of 80 ± 10, 65 ± 15, 75 ± 15, and 60 ± 10 μm, respectively, which were not changed significantly by MeOH treatment. As silk fibroin concentrations used to cast the film were standardized, differences in film thickness depended only on the initial volumes of silk
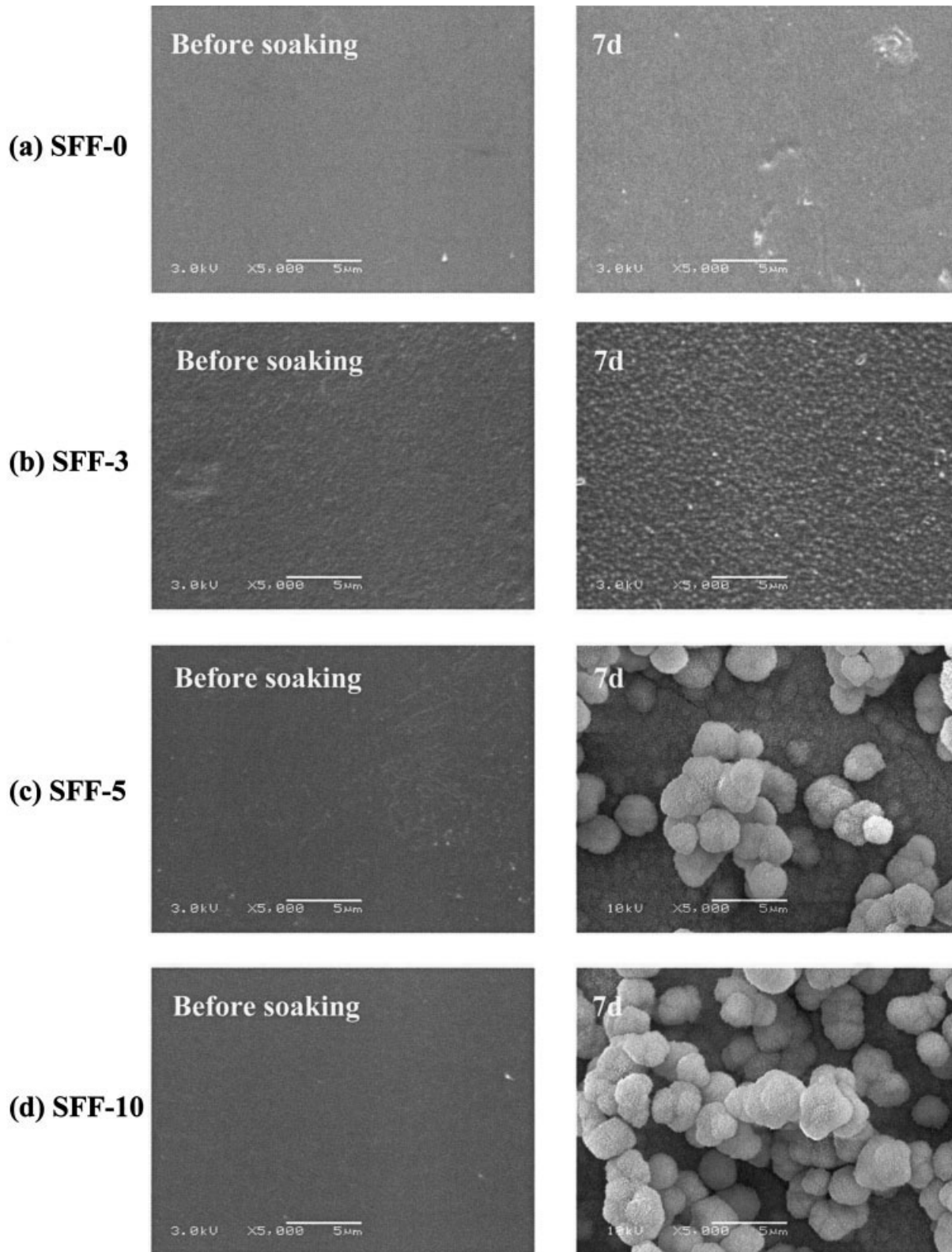
Figure 3 SEM images of the SFF surfaces before and after soaking in 1.5 SBF at 7 days; (a) SFF-0, (b) SFF-3, (c) SFF-5 and (d) SFF-10.

fibroin solutions. The transmittances at 500 nm for each film were 87.7 ± 0.18, 87.4 ± 0.13, 88.1 ± 0.09, and 86.8 ± 0.11%, respectively, and the SFFs showed transmissions over 85% in the visible range.

Figure 1 shows FTIR-ATR spectra between 1600 and 1700 cm^{-1} of the SFFs before and after the MeOH treatment to determine the conformational changes. The amide I band, observed at 1600–1700cm^{-1} is gen-

erally used for conformational determination. The following assignments are generally used: α-helical structure, $1660-1650 cm^{-1}$; random coil structure, $1650-1640 cm^{-1}$; and β-sheet, $1640-1620 cm^{-1}$.[22,23] The SFFs before the MeOH treatments clearly have one symmetrical peak at $1651 cm^{-1}$. The width of the band, however, increases with increasing the concentrations of calcium ions. Thus, the SFFs before the MeOH treatment could have an approximately on equal mixture of α-helical structure and random coil, commonly observed in SFFs cast at $20-40°C$ on a PS substrate. Casting silk fibroin solutions at higher temperature than $40°C$, SFFs gave a β-sheet structure with the IR peak at $1626 cm^{-1}$.[22]

The calcium ions affect the conformational transition from the α-helical or the intermediate with random coil to the β-sheet structure.[21] The effect of calcium ion concentration and pH value on the conformational changes have been clearly described from NMR and Raman analyses by Freddi et al.,[21] over the pH range from 6.9 to 8.0. As the calcium ion concentration range from 0 to 10 wt % relative to the silk fibroin, the random coil predominated. Over this range of calcium ion concentration, the proportion of α-helical and β-sheet structures changes, and the maximum β-sheet content occurs at 1 wt % of calcium ions.[21] In the present study, using SFFs with calcium concentration over 3 wt % per silk fibroin, the observed conformational contents were in good agreement with the findings of Freddi et al.[21]

The MeOH treatment caused the split of the band at $1651 cm^{-1}$ into two peaks at 1651 and $1626 cm^{-1}$; the latter peak attributed to β-sheet was almost coincident with that observed in previous studies.[18] The intensity of the band at $1626 cm^{-1}$ became dominant with increasing calcium ion concentration. Thus, the stability of β-sheet structure was improved by the inclusion of calcium ions in the film and by subsequent MeOH treatment.

The effect of calcium chloride concentrations in silk fibroin films on hydroxyapatite deposition

Figure 2 shows the XRD patterns of SFF-0, SFF-3, SFF-5, and SFF-10 after soaking in 1.5 SBF for 7 days. The broad diffraction at 20.0 degrees (2θ) in each pattern was attributed to the crystalline regions of β-sheet structure of silk fibroin. The XRD patterns indicate that SFF-0 and SFF-3 did not mineralize with the hydroxyapatite crystals. Many authors have studied how chemical modification of silk fibroin fabrics can improve their ability to mineralize with hydroxyapatite.[9,41] Our method is far simpler requiring only the addition of 5 g $CaCl_2$/100 g fibroin to enhance the subsequent deposition of hydroxyapatite.

SFF-5 and SFF-10, compared with SFF-0 and SFF-3, gave additional diffractions (25.9 and 32 degrees (2θ))
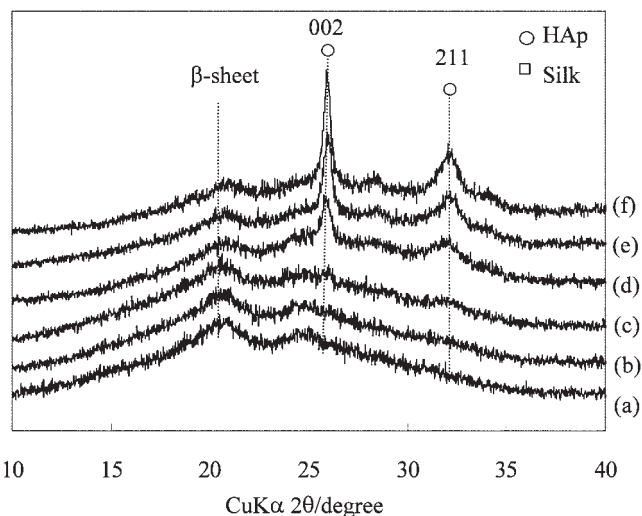

Figure 4 XRD patterns of (a) SFF-5 before soaking and those soaked into 1.5 SBF for (b) 3 h, (c) 6 h, (d) 12 h, (e) 1 day, (f) 3 days and (g) 7 days.

assigned, respectively, to (002) and (211) of hydroxyapatite crystals. The intensity ratio of these diffractions was not matched to the pure hydroxyapatite. This might suggest the presence of octacalcium phosphate ($Ca_8H_2(PO_4)_6 5H_2O$; OCP) and/or the obtained hydroxyapatite crystals resulted in the hydrolysis of OCP. The characteristic diffraction attributed to the OCP at 9.3 degree (2θ) was not observed (data not shown). However, many authors have reported that OCP is initially formed from SBF.[46,47] Our study also supports the hypothesis that hydroxyapatite crystals are formed from OCP. The intensities of (211) and (002) increased with the concentrations of calcium ions added to the SFF, indicating the increasing hydroxyapatite deposition.

Figure 3 shows the SEM images of the SFF-0, SFF-3, SFF-5, and SFF-10 before and after soaking in 1.5 SBF at pH of 7.25 at 36.5°C for 7 days. The SFFs before soaking in 1.5 SBF had a smooth surface. SFF-0 and SFF-3 showed no surface changes. In contrast, the surface of SFF-5 and SFF-10 showed small (50–100 nm-long and 10-nm-thick) petal-shaped crystals at 7 days, and with time, these aggregated into 2–3 μm irregularly spherical. The number of aggregates increased with the concentrations of calcium ions in the SFF. XRD confirms this observation and strongly suggests that the aggregates be composed of hydroxyapatite.

The effect of soaking time on hydroxyapatite deposition

Figure 4 shows the XRD patterns of SFF-5 after soaking in 1.5 SBF for 3, 6, 12, 24 h and 7 days. The broad diffractions from the crystalline β-sheet structure of
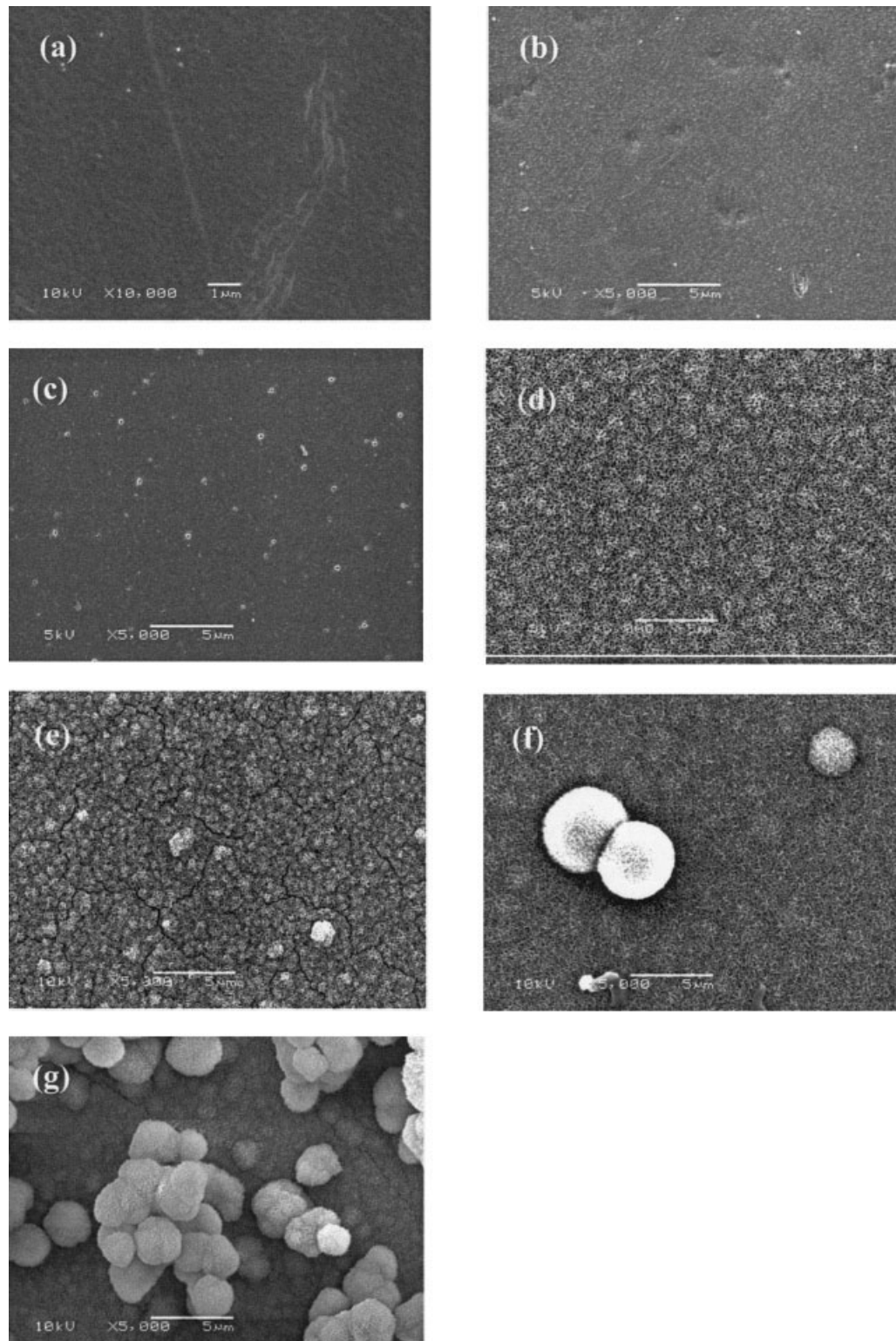
Figure 5 SEM images of the SFF-5 surfaces (a) before soaking and after soaking in 1.5 SBF for (b) 3 h, (c) 6 h, (d) 12 h, (e) 1 day, (f) 3 days, (g) 7 days.

silk fibroin were observed at 20° in each pattern. The diffractions from the deposited hydroxyapatite were detected at 25.9 and 32.0 degrees after soaking for 6 h. The FTIR spectra of these samples (data not shown)

showed that phosphate ions at ~1030 cm^{-1} appeared after soaking for 3 h, probably indicating the formation of OCP or hydroxyapatite. The intensity ratio of the diffractions attributed to the hydroxyapatite also
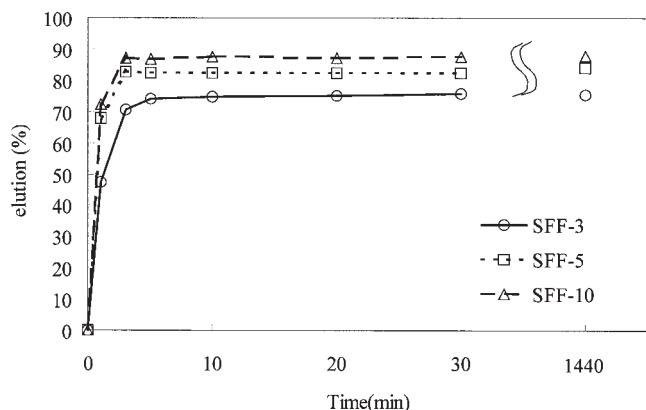
Figure 6 The elution of Ca ion from the SFFs to ultra-pure water against the soaking times.

indicated the conversion of hydroxyapatite from OCP. The intensity of hydroxyapatite diffractions increased with soaking times, and thus, the thickness of hydroxyapatite deposited layer could be regulated by soaking times.

Figure 5 shows the SEM images of SFF-5 surfaces after soaking in 1.5 SBF for 3, 6, 12, and 24 h and 7 days. After 3 h, the hydroxyapatite crystals could not be seen yet. At 6 h, the dots with 200–300 nm in diameter attributed to the OCP or hydroxyapatite crystals first appeared. At 12 h, the petal-shaped hydroxyapatite crystals (10–50-nm-long and 10-nm-thick) evenly covered the surface of SFF. Soaking in 1.5 SBF for 12 h promoted the formation of irregularly spherical aggregates of hydroxyapatite evenly covering the SFF surface. Finally, large spherical aggregates of hydroxyapatite crystals appeared on the SFF surface. Similar findings have been described by several authors.[9,33]

Calcium ion elution from silk fibroin films in water and removed form 1.5 SBF

Figure 6 shows the time course of elution of calcium ions in ultrapure water from the unmineralized SFF-3, SFF-5. The calcium ions in the supernatant liquids were analyzed by ICP measurements. Leaching of calcium ion commenced immediately after immersion and reached a plateau of 70–90% of the starting calcium ions. The calcium ions were probably stabilized on the β-sheet structure of the silk fibroin.[48,49] In this study, the addition of calcium ions increased the portion of β-sheet structure. The calcium ions, however, were not tightly bonded to the β-sheet structure, as they eluted rapidly from the SFFs. *Bombyx mori* heavy chain fibroin has an estimated pH of 4.4 resulting from the strong preponderance of amino acids with a carboxyl side chain. Of this, glutamic acid is concentrated in the

N-terminal peptide while most of the hydrophilic spacers in the massive repetitive central region contain two aspartic acid residues in close proximity. The rather even arrangement of the hydrophilic spacer along the length of the central core region together with their negatively charged carboxyl groups probably makes excellent low affinity bonding site for calcium ions to nucleate the formation of OCP.

Figure 7 shows the effect of time on the concentration of Ca^{2+} and HPO_4^{2-} ions remaining in the 1.5 SBF containing SFF-5 or SFF-10 as measured with ICP. The initial concentrations of 1.5 SBF in: 3.75 mM of Ca^{2+}; 1.50 mM of HPO_4^{2-}; 212.78 mM of Na^+; and 7.50 mM of K^+. The concentrations of Na^+ and K^+ ions remained constant throughout soaking for SFF-5 and SFF-10. The concentrations of calcium ion for SFF-5 and SFF-10 increased at 0.42 and 0.87 mM. There was a lag period of about an hour before the phosphate ion concentrations started to fall probably resulting from the slow formation of nucleation sites. We can calculate the compositions of hydroxyapatite deposited on the SFF surfaces at a
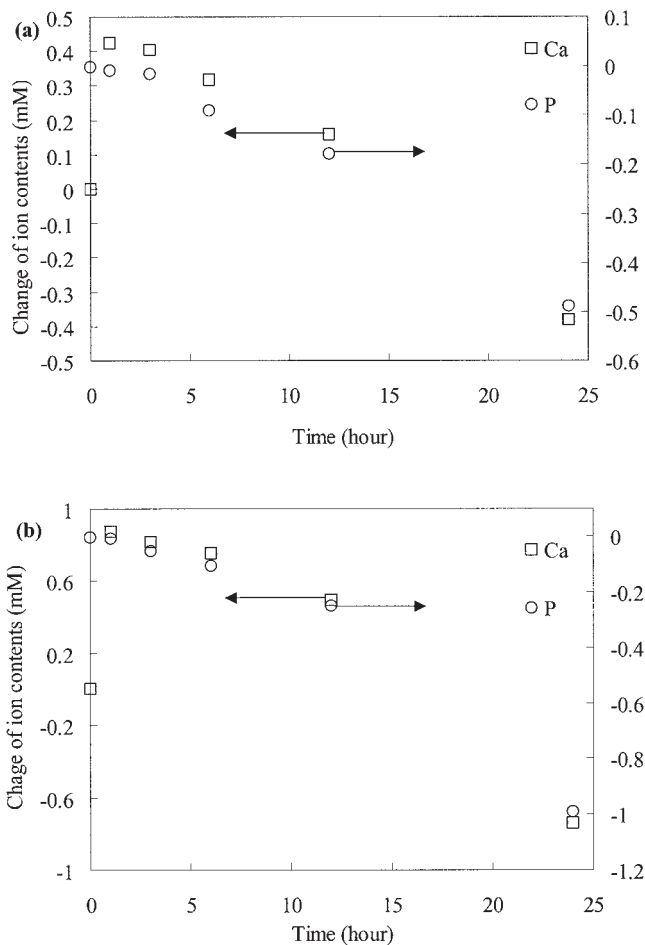

Figure 7 The change of ion content of Ca^{2+} and HPO_4^{2-} ions in 1.5 SBF against soaking times; (a) SFF-5 (b) SFF-10.

given time from the changes in concentration by subtracting the concentrations of Ca^{2+} and HPO_4^{2-} ions at 1 h. After soaking for 3 h, the concentrations of Ca^{2+} and HPO_4^{2-} ions decreased to 0.019 and 0.017 mM for SFF-5, and 0.057 and 0.052 mM for SFF-10. The Ca/P ratio was, then, calculated to be 1.10 for mineral deposited on SFF-5 and SFF-10 and 1.15 and 1.12 for SFF-5 and SFF-10 at 6 h. This suggests the deposition of OCP (Ca/P ratio of 1.33) or a calcium deficient hydroxyapatite instead of hydroxyapatite (Ca/P ratio of 1.67) in the early stages of mineralization. This is in line with our XRD observations and other published findings.[46,47] The lack of $CaHPO_4$ and $CaHPO_42H_2O$ in the mineralization may result from the constant pH of 7.25 of 1.5 SBF.

After 12 and 24 h in 1.5 SBF, the Ca/P ratio increased to 1.48 and 1.65 for SFF-5, and 1.52 and 1.63 for SFF-10, respectively, approaching the value of 1.67 for hydroxyapatite. The change of the Ca/P ratio indicates that the calcium phosphate crystals with the low Ca/P ratio were initially deposited and this was replaced by hydroxyapatite with time.

CONCLUSIONS

Transparent silk fibroin films containing various calcium chloride contents were prepared by casting from aqueous solutions. The stability of β-sheet structure was improved by the addition of calcium ions and the subsequent MeOH treatment. Silk fibroin films containing >5 wt % calcium chloride become coated with hydroxyapatite crystals after soaking in 1.5 SBF for 6 h, while controls containing less calcium did not. Changes in the mineralization with time were followed by XRD and by changes in the composition of 1.5 SBF soaking the silk fibroin films. This confirmed that the initial mineralization is by OCP, which is subsequently converted to hydroxyapatite. These findings suggest that the simple addition of calcium ions to regenerated silk fibroin may provide a useful method for producing hydroxyapatite-mineralized materials for bone repair.

References

1. Altman, G. H.; Diaz, F.; Jakuba, C.; Calabro, T.; Horan, R. L.; Chen, J.; Lu, H.; Richmond, J.; Kaplan, D. L. Biomaterials 2003, 24, 401.
2. Asakura, T.; Kaplan, D. L. In Encylopedia Agriculatural Science; Arntzen, C. J., Ritter, E. M. Eds.; Academic Press: New York 1994; Vol. 4, p 1.
3. Nazarov, R.; Jin, H. J.; Kaplan, D. L. Biomacromolecules 2004, 5, 718.
4. Zaoming, W.; Codina, R.; Fernandez, Caldas, E.; Lockey, F.; Bukanz, S. C. J Allerg Clinic Immunol 1996, 97, 109.
5. Panilaitis, B.; Altman, G. H.; Chen, J.; Jin, H. J; Karageorgiou, V; Kaplan, D. L. Biomaterials 2003, 24, 3079.
6. Santin, M.; Motta, A.; Freddi, G.; Cannas, M. J Biomed Mater Res 1999, 46, 382.
7. Jin, H. J; Chen, J. S.; Karageorgiou, V.; Altman, G. H.; Kaplan, D. L. Biomaterials 2004, 25, 1039.
8. Unger, R. E.; Peters, K.; Wolf, M.; Motta, A.; Migliaresi, C.; Kirkpatrick, C. J Biomaterials 2004, 25, 5137.
9. Tamada, Y.; Furuzono, T.; Taguchi, T.; Kishida, A.; Akashi, M. Biomat Sci Poly Edn 1999, 10, 787.
10. Aoki, H.; Tomita, N.; Morita, Y.; Hattori, K.; Harada, Y.; Sonobe, M.; Wakitani, S.; Tamada Y. Bio-Med Mater Eng 2003, 13, 309.
11. Kweon, H.; Ha, H. C.; Um, I. C.; Park, Y. H. J Appl Polym Sci 2001, 80, 928.
12. Altman, G. H.; Lu, H. H.; Horan, R. L.; Calabro, T.; Ryder, D.; Kaplan, D. L.; Stark, P.; Martin, I.; Richmond, J. C.; Vunjak-Novakovic, G. J Biomech Eng 2002, 124, 742.
13. Arai, T.; Freddi, G.; Innocenti, R.; Tsukada, M. J Appl Polym Sci 2004, 91, 2383.
14. Li, M. Z.; Ogiso, M.; Minoura, N. Biomaterials 2003, 24, 357.
15. Minoura, N.; Tsukada, M.; Nagura, M. Biomaterials 1990, 11, 430.
16. Lam, K. H.; Nijenhuis, A. J.; Bartels, H.; Postema, A. R.; Jonkman, M. F.; Pennings, A. J.; Nieuwenhuis, P. J Appl Biomater 1995, 6, 191.
17. Greenwald, D.; Shumway, S.; Albear, P.; Gottlieb, L. J Surg Res 1994, 56, 372.
18. Magishi, J; Nakamura, S. J Polym Sci Part B 1985, 23, 227.
19. Tsukada, M.; Freddi, G.; Monti, P.; Bertoluzza, A.; Kasai, N. J Polym Sci Part B 1995, 33, 1995.
20. Tsukada, M.; Freddi, G.; Gotoh, Y.; Kasai, N. J Polym Sci Part B 1994, 32, 1407.
21. Freddi, G.; Monti, P.; Nagura, M.; Gotoh, Y.; Tsukada, M. J Polym Sci Part B 1997, 35, 841.
22. Zhou, P.; Xie, X.; Knight, D. P.; Zong, X. H.; Feng, D.; Yao, W. H. Biochemistry 2004, 43, 11302.
23. Tretinnikov, O. N.; Tamada, Y. Langmuir 2001, 17, 7406.
24. Surewcz, W. K.; Mantsch, H. H. Biomedica et Biophysyca Acta 1988, 952, 115.
25. Noishiki, Y.; Nishiyama, Y.; Wada, M.; Kuga, S.; Magoshi, J. J Appl Polym Sci 2002, 86, 3425.
26. Altman, G. H.; Horan, R.; Moreau, J.; Martin, I.; Richmond, J.; Kaplan, D. L. Biomaterials 2002, 23, 4131.
27. Li, G. Y.; Zhou, P.; Sun, Y. J.; Yao, W. H.; Mi, Y.; Yoa, H. Y.; Shao, Z. Z.; Yu, T. Y. Chem J Chin Univ 2001, 2, 860.
28. Min, B. M.; Lee, G.; Kim, S. H.; Nam, Y. S.; Lee, T. S.; Park, W. H. Biomaterials 2004, 25, 1289.
29. Hanker, J. S.; Giammara, B. L. Science 1988, 242, 885.
30. Walsh, W. R.; Ohno, M.; Guzelsu, N. J Mater Sci Mater Med 1994, 5, 72.
31. Ohashi, H.; Therin, M.; Meunier, A.; Christel, P. J Mater Sci Mater Med 1994, 5, 237.
32. Gineste, L.; Gineste, M.; Ranz, X.; Ellefterion, A.; Guilhem. A.; Rouquet, N.; Frayssinet, P. J Biomed Mater Res 1999, 48, 224.
33. Kikuchi, M.; Itoh, S.; Ichinose, S.; Shinomiya, K.; Tanaka, J. Biomaterials 2001, 22, 1705.
34. Zhang, L. J; Feng, X. S.; Liu, H. G.; Qian, D. J.; Zhang, L.; Yu, X. L.; Cui, F. Z. Mater Let 2004, 58, 719.
35. Wu, T. J.; Huang, H. H.; Lan, C. W.; Lin, C. H.; Hsu, F. Y.; Wang, Y. J. Biomaterials 2004, 25, 651.
36. Tampieri, A.; Celotti, G.; Landi, E.; Sandri, M.; Roveri, N.; Falini, G. J Biomed Mater Res Part A 2003, 67A, 618.
37. Mythili, J; Sastry, T. P.; Subramanian, M. Biotech Appl Biochem 2000, 32, 155.
38. Du, C.; Cui, F. Z.; Zhang, W.; Feng, Q. L.; Zhu, X. D.; de Groot, K. J Biomed Mater Res 2000, 50, 518.

39. Du, C.; Cui, F. Z.; Zhu, X. D.; de Groot, K. J Biomed Mater Res 1999, 44, 407.

40. Zhao, F.; Yin, Y. J.; Lu, W. W.; Leong, J. C.; Zhang, W.; Zhang, J. Y.; Zhang, M. F.; Yao, K. D. Biomaterials 2002, 23, 3227.

41. Furuzono, T.; Taguchi, T.; Kishida, A.; Akashi, M.; Tamada, Y. J Biomed Mater Res 2000, 50, 344.

42. Combes, C.; Rey, C. Biomaterials 2002, 23, 2817.

43. Kim, H. M.; Miyaji, F.; Kokubo, T.; Nakamura, T. J Biomed Mater Res 1996, 32, 409.

44. Ohgo, K.; Zhao, C. H.; Kobayashi, M.; Asakura, T. Polymer 2003, 44, 841.

45. Kokubo, T.; Ito, S.; Huang, Z. T.; Tanahashi, T.; Sakka, S.; Kitsugi, T.; Yamamoto, T. J Biomed Mater Res 1990, 24, 331.

46. Lin, S. J; LeGeros, R. Z.; Le, Geros, J. P. J Biomed Mater Res Part A 2003, 66A. 819.

47. Miake, Y.; Yanagisawa, T.; Yajima, Y.; Noma, H.; Yasui, N.; Nonami, T. J Dental Res 1995, 74, 1756.

48. Ochi, A.; Hossain, K. S.; Magoshi, J.; Nemoto, N. Biomacromolecules 2002, 3, 1187.

49. Hossain, K. S.; Ochi, A.; Ooyama, E.; Magoshi, J.; Nemoto, N. Biomacromolecules 2003, 4, 350.